

Gutzwiller Method for an Extended Periodic Anderson Model with the c - f Coulomb Interaction

Katsunori KUBO

Advanced Science Research Center, Japan Atomic Energy Agency, Tokai, Ibaraki 319-1195

(Received August 11, 2011; accepted August 25, 2011; published online October 17, 2011)

We study an extended periodic Anderson model with the Coulomb interaction U_{cf} between conduction and f electrons by the Gutzwiller method. The crossovers between the Kondo, intermediate-valence, and almost empty f -electron regimes become sharper with U_{cf} , and for a sufficiently large U_{cf} , become first-order phase transitions. In the Kondo regime, a large enhancement in the effective mass occurs as in the ordinary periodic Anderson model without U_{cf} . In addition, we find that a large mass enhancement also occurs in the intermediate-valence regime by the effect of U_{cf} .

KEYWORDS: mass enhancement, Gutzwiller approximation, extended periodic Anderson model, valence transition, valence fluctuations, heavy-fermion superconductivity

1. Introduction

In rare-earth and actinide compounds, several interesting phenomena, such as magnetism, heavy-fermion phenomena, and superconductivity, occur owing to the interplay of the strong Coulomb interaction U between f electrons and the hybridization V between the localized f -orbital and conduction band.

Among such phenomena, heavy-fermion superconductivity has been one of the central issues in f -electron physics after the discovery of the superconductivity in CeCu_2Si_2 .¹⁾ In the heavy-fermion systems, the conventional, phonon-mediated, s -wave superconductivity is hardly realized owing to the strong onsite Coulomb interaction. Then, pairing mechanisms other than the phonon-mediated mechanism have been discussed. The magnetic-fluctuation-mediated superconducting mechanism may be common in heavy-fermion superconductors, since superconductivity is realized near a magnetic quantum critical point in many compounds.

However, some heavy-fermion superconductors are difficult to understand solely by the magnetic fluctuation scenario. For example, the superconducting transition temperatures under pressure in CeCu_2Si_2 ²⁾ and CeCu_2Ge_2 ,³⁾ become maximum far away from the magnetic quantum critical points. In $\text{CeCu}_2\text{Si}_{1.8}\text{Ge}_{0.2}$,⁴⁾ the superconducting region splits into two regions: the low-pressure region close to the magnetic critical point and the high-pressure region away from the magnetic critical point. To explain the high-pressure superconducting phase, a valence fluctuation scenario is proposed⁵⁻⁸⁾ and the importance of the Coulomb interaction U_{cf} between conduction and f electrons has been discussed in addition to U and V .

Valence fluctuations are expected from the rapid change in the valence of an f ion in these compounds under pressure, which is suggested from the behavior of the effective mass m^* . In the periodic Anderson model (PAM), m^* and the number of electrons, n_f , in the f orbital per site follow the relation^{9,10)}

$$\frac{m^*}{m} = \frac{1 - n_f/2}{1 - n_f}, \quad (1)$$

where m is the free-electron mass. This relation is derived using the Gutzwiller method for $U \rightarrow \infty$. Thus, a large change in m^* indicates a large change in n_f . For CeCu_2Si_2

and CeCu_2Ge_2 , m^* is experimentally deduced from specific heat measurements or the temperature dependence of electrical resistivity, and it is found that m^* decreases rapidly at approximately the pressure where the superconducting transition temperature becomes maximum.^{11,12)} Thus, these observations indicate that a sharp valence change or large valence fluctuations play important roles in superconductivity.

However, there are problems with the relation between the effective mass and valence. First, eq. (1) is derived for an ordinary PAM, which does not show a sharp valence change. Thus, we cannot naively apply eq. (1) to a system with large valence fluctuations. Second, the effective mass has a peak in CeCu_2Si_2 under pressure before the superconducting transition temperature becomes maximum, that is, the effective mass varies nonmonotonically under pressure.¹²⁾ This nonmonotonic variation in the effective mass cannot be explained by eq. (1), since the n_f of a Ce ion is expected to decrease monotonically under pressure for the following reasons. A positively charged Ce ion should be surrounded by negative charges. When these negative charges get close to a Ce ion under pressure, the f level ϵ_f of Ce is lifted. Under pressure, the overlap between the wave functions of the f orbital and the conduction band increases, and V increases. Both the effects of pressure on ϵ_f and V result in a decrease in n_f . Indeed, a monotonic decrease in n_f under pressure has been observed in CeCu_2Si_2 by an X-ray absorption experiment recently.¹³⁾ We also note that, in CeCu_2Ge_2 , the pressure dependence of the effective mass has a shoulder structure before the superconducting transition temperature becomes maximum.¹¹⁾ This shoulder structure may also become a peak as in CeCu_2Si_2 , if we subtract the contributions of magnetic fluctuations, which are large in the low-pressure region.

The peak structures in the effective mass may be explained by considering a combined effect of the renormalization described by eq. (1) and valence fluctuations.¹²⁾ However, the applicability of eq. (1) to a system with large valence fluctuations is not justified. Thus, it is an interesting problem how eq. (1) can be extended to a model that shows a sharp valence change. A study of such a problem will be helpful to understand superconductivity in CeCu_2Si_2 and CeCu_2Ge_2 by the valence fluctuation scenario.

Note that heavy-fermion behaviors in α - YbAlB_4 and β -

YbAlB_4 ¹⁴⁾ are also difficult to explain by eq. (1). The valences of the Yb ion are +2.73 for α -YbAlB₄ and +2.75 for β -YbAlB₄,¹⁵⁾ that is, the hole numbers of Yb ions are $n_f = 0.73$ and 0.75 for α -YbAlB₄ and β -YbAlB₄, respectively. For these values of n_f , i.e., much less than unity, we cannot expect heavy-fermion behavior from eq. (1).

In this research, we study an extended periodic Anderson model (EPAM) with the Coulomb interaction U_{cf} between conduction and f electrons by the Gutzwiller method. We extend the Gutzwiller method for the PAM developed by Fazekas and Brandow¹⁰⁾ to the present model. Then, we investigate the effect of U_{cf} on the effective mass. Although the EPAM has been studied as a typical model for valence transition¹⁶⁾ and has been investigated by some modern techniques in recent years^{6-8,17-19)} after the proposal of the valence fluctuation scenario for superconductivity, the effect of U_{cf} on the mass enhancement has not been clarified well. Some of the results have already been reported in our previous paper;²⁰⁾ here, we report the details of the method and also add new results.

2. Formulation

The EPAM is given by¹⁶⁾

$$\begin{aligned}
 H = & \sum_{k\sigma} \epsilon_k c_{k\sigma}^\dagger c_{k\sigma} + \epsilon_f \sum_{r\sigma} n_{fr\sigma} \\
 & - V \sum_{k\sigma} (f_{k\sigma}^\dagger c_{k\sigma} + c_{k\sigma}^\dagger f_{k\sigma}) \\
 & + U \sum_r n_{fr\uparrow} n_{fr\downarrow} + U_{cf} \sum_{r\sigma\sigma'} n_{c r\sigma} n_{f r\sigma'},
 \end{aligned} \quad (2)$$

where $c_{k\sigma}$ and $f_{k\sigma}$ are the annihilation operators of conduction and f electrons, respectively, with the momentum \mathbf{k} and the spin σ . $n_{c r\sigma}$ and $n_{f r\sigma}$ are the number operators at site \mathbf{r} with σ of the conduction and f electrons, respectively. ϵ_k is the kinetic energy of the conduction electron. We have not taken orbital degrees of freedom into consideration. This simplification may be justified for a system with tetragonal symmetry such as CeCu₂Si₂ and CeCu₂Ge₂ and for a system with orthorhombic symmetry such as α -YbAlB₄ and β -YbAlB₄, since the crystalline electric field ground states of f electrons are Kramers doublets in these systems. In the following, we set the energy level of the conduction band as the origin of energy, i.e., $\sum_k \epsilon_k = 0$. We set $U \rightarrow \infty$, since the onsite Coulomb interaction between well-localized f electrons is large.

We consider the variational wave function given by

$$|\psi\rangle = P_{ff} P_{cf} |\phi\rangle, \quad (3)$$

where

$$P_{ff} = \prod_r [1 - n_{fr\uparrow} n_{fr\downarrow}] \quad (4)$$

excludes the double occupancy of f electrons at the same site, and

$$P_{cf} = \prod_{r\sigma\sigma'} [1 - (1 - g) n_{c r\sigma} n_{f r\sigma'}] \quad (5)$$

is introduced to deal with the onsite correlation between conduction and f electrons.¹⁷⁾ g is a variational parameter. The

one-electron part of the wave function is given by

$$|\phi\rangle = \prod_{k < k_F, \sigma} [c_{k\sigma}^\dagger + a(\mathbf{k}) f_{k\sigma}^\dagger] |0\rangle, \quad (6)$$

where k_F is the Fermi momentum for the free conduction band without f electrons, $|0\rangle$ denotes vacuum, and $a(\mathbf{k})$ is determined variationally. Here, we have assumed that the total number n of electrons per site is less than 2.

In the method by Fazekas and Brandow,¹⁰⁾ the f -electron state is expanded in the basis state in real space, since it is convenient to deal with the projection operator P_{ff} . In the present study, we consider P_{cf} in addition to P_{ff} , and thus we also expand the conduction-electron state in real space. This is the main difference from the method of Fazekas and Brandow. The creation operator is expanded as

$$b_{\mathbf{k}}^\dagger = \frac{1}{\sqrt{L}} \sum_r e^{i\mathbf{k}\cdot\mathbf{r}} b_{\mathbf{r}}^\dagger = \sum_r \varphi_{\mathbf{k}}(\mathbf{r}) b_{\mathbf{r}}^\dagger, \quad (7)$$

where L is the number of lattice sites and b denotes c_σ or f_σ . Then, the basis state in momentum space is expanded as

$$\begin{aligned}
 | \{ \mathbf{k}^{(b)} \} \rangle &= \prod_{i=1}^{N_b} b_{\mathbf{k}_i}^\dagger |0\rangle \\
 &= \sum_{\{ \mathbf{r}^{(b)} \}} \det[\varphi_{\mathbf{k}^{(b)}}(\mathbf{r}^{(b)})] \prod_{i=1}^{N_b} b_{\mathbf{r}_i}^\dagger |0\rangle \\
 &= \sum_{\{ \mathbf{r}^{(b)} \}} \det[\varphi_{\mathbf{k}^{(b)}}(\mathbf{r}^{(b)})] | \{ \mathbf{r}^{(b)} \} \rangle.
 \end{aligned} \quad (8)$$

The determinant is defined as

$$\det[\varphi_{\mathbf{k}}(\mathbf{r})] = \begin{vmatrix} \varphi_{k_1}(\mathbf{r}_1) & \varphi_{k_1}(\mathbf{r}_2) & & \\ \varphi_{k_2}(\mathbf{r}_1) & \varphi_{k_2}(\mathbf{r}_2) & & \\ & & \ddots & \\ & & & \varphi_{k_{N_b}}(\mathbf{r}_{N_b}) \end{vmatrix}. \quad (9)$$

The basis state including both c and f electrons is given by

$$| \{ \mathbf{r}^{(c)} \} \{ \mathbf{r}^{(f)} \} \rangle = \prod_\sigma \prod_{j=1}^{N_{c\sigma}} c_{\mathbf{r}_j^{(c\sigma)}}^\dagger \prod_{i=1}^{N_{f\sigma}} f_{\mathbf{r}_i^{(f\sigma)}}^\dagger |0\rangle, \quad (10)$$

where $N_{c\sigma}$ and $N_{f\sigma}$ are the numbers of conduction and f electrons, respectively, with spin σ . The total number of spin- σ electrons, $N_\sigma = N_{c\sigma} + N_{f\sigma}$, should be fixed. Here, we have introduced the notation $\{ \mathbf{r}^{(c)} \} = \{ \mathbf{r}^{(c\uparrow)}, \mathbf{r}^{(c\downarrow)} \}$ and $\{ \mathbf{r}^{(f)} \} =$

$\{\mathbf{r}^{(f\uparrow)}, \mathbf{r}^{(f\downarrow)}\}$. Then, the one-particle part is expanded as

$$\begin{aligned}
|\phi\rangle &= \prod_{\sigma} \sum_{N_{f\sigma}, \{\mathbf{k}^{(f\sigma)}\}} (-1)^{\text{perm}(\{\mathbf{k}^{(f\sigma)}\})} \\
&\times \prod_{j=1}^{N_{c\sigma}} c_j^{\dagger} \prod_{i=1}^{N_{f\sigma}} a(\mathbf{k}_i^{(f\sigma)}) f_{\mathbf{k}_i^{(f\sigma)}}^{\dagger} |0\rangle \\
&= \prod_{\sigma} \sum_{N_{f\sigma}, \{\mathbf{k}^{(f\sigma)}\}} (-1)^{\text{perm}(\{\mathbf{k}^{(f\sigma)}\})} \\
&\times \prod_{i=1}^{N_{f\sigma}} a(\mathbf{k}_i^{(f\sigma)}) \\
&\times \sum_{\{\mathbf{r}^{(c\sigma)}, \{\mathbf{r}^{(f\sigma)}\}\}} \det[\varphi_{\mathbf{k}^{(c\sigma)}}(\mathbf{r}^{(c\sigma)})] \det[\varphi_{\mathbf{k}^{(f\sigma)}}(\mathbf{r}^{(f\sigma)})] \\
&\times |\{\mathbf{r}^{(c)}\}\{\mathbf{r}^{(f)}\}\rangle,
\end{aligned} \tag{11}$$

where $(-1)^{\text{perm}(\{\mathbf{k}^{(f\sigma)}\})}$ is the sign due to the fermion anti-commutation relation. In the summation, we should keep $k_j^{(c\sigma)}, k_i^{(f\sigma)} < k_F$ and $\{\mathbf{k}^{(c\sigma)}\} \cap \{\mathbf{k}^{(f\sigma)}\} = \emptyset$. Then the projection in eq. (3) is carried out by restricting the summation in eq. (11) with the condition $\{\mathbf{r}^{(f\uparrow)}\} \cap \{\mathbf{r}^{(f\downarrow)}\} = \emptyset$ and by multiplying each term by g^D . $D = D_{c\uparrow} + D_{c\downarrow}$, where $D_{c\sigma}$ is the number in the set $\{\mathbf{r}^{(c\sigma)}\} \cap \{\mathbf{r}^{(f)}\}$. That is, D is the number of interacting electron pairs through U_{cf} . In the following formulation, we impose these restrictions without mentioning them explicitly.

Then, we evaluate the normalization factor $\langle\psi|\psi\rangle$ using the approximation introduced in Appendix A. By using eq. (A-4), we obtain

$$\begin{aligned}
\langle\psi|\psi\rangle &\simeq \sum_{N_{f\uparrow}N_{f\downarrow}} \sum_{\{\mathbf{k}^{(f)}\}} \prod_{i=1}^{N_{f\uparrow}} a^2(\mathbf{k}_i^{(f\uparrow)}) \prod_{j=1}^{N_{f\downarrow}} a^2(\mathbf{k}_j^{(f\downarrow)}) \\
&\times \sum_{\{\mathbf{r}\}} g^{2D} |\det[\varphi_{\mathbf{k}^{(c\uparrow)}}(\mathbf{r}^{(c\uparrow)})]|^2 |\det[\varphi_{\mathbf{k}^{(f\uparrow)}}(\mathbf{r}^{(f\uparrow)})]|^2 \\
&\times |\det[\varphi_{\mathbf{k}^{(c\downarrow)}}(\mathbf{r}^{(c\downarrow)})]|^2 |\det[\varphi_{\mathbf{k}^{(f\downarrow)}}(\mathbf{r}^{(f\downarrow)})]|^2,
\end{aligned} \tag{12}$$

where $\{\mathbf{k}^{(f)}\} = \{\mathbf{k}^{(f\uparrow)}, \mathbf{k}^{(f\downarrow)}\}$ and $\{\mathbf{r}\} = \{\mathbf{r}^{(c)}, \mathbf{r}^{(f)}\}$. By applying eq. (A-3), we further approximate $\langle\psi|\psi\rangle$ and obtain

$$\begin{aligned}
\langle\psi|\psi\rangle &\simeq \sum_{N_{f\uparrow}N_{f\downarrow}D_{c\uparrow}D_{c\downarrow}} g^{2D} X(N_{f\uparrow}, N_{f\downarrow}) \\
&\times Y(N_f, N_{c\uparrow}, D_{c\uparrow}) Y(N_f, N_{c\downarrow}, D_{c\downarrow}) \\
&\times Z(N_{f\uparrow}) Z(N_{f\downarrow}),
\end{aligned} \tag{13}$$

where $N_f = N_{f\uparrow} + N_{f\downarrow}$,

$$X(N_{f\uparrow}, N_{f\downarrow}) = \frac{L^{-N_{f\uparrow}} C_{N_{f\downarrow}}}{L C_{N_{f\downarrow}}}, \tag{14}$$

$$Y(N_f, N_{c\sigma}, D_{c\sigma}) = \frac{N_f C_{D_{c\sigma}} L^{-N_f} C_{N_{c\sigma} - D_{c\sigma}}}{L C_{N_{c\sigma}}}, \tag{15}$$

and

$$\begin{aligned}
Z(N_{f\sigma}) &= \sum_{\{\mathbf{k}^{(f\sigma)}\}} \prod_{i=1}^{N_{f\sigma}} a^2(\mathbf{k}_i^{(f\sigma)}) \\
&= \sum_{\{\mathbf{k}^{(f\sigma)}\}} \exp\left\{-\sum_{i=1}^{N_{f\sigma}} [-\ln a^2(\mathbf{k}_i^{(f\sigma)})]\right\} \\
&= \exp[-F(N_{f\sigma})].
\end{aligned} \tag{16}$$

$Z(N_{f\sigma})$ is the partition function of the canonical ensemble for the system with the dispersion $\varepsilon_{\mathbf{k}} = -\ln a^2(\mathbf{k})$ with the constraint $k < k_F$ at temperature 1. $F(N_{f\sigma})$ is the free energy of this fictitious system. Then, by using the Stirling formula, we rewrite the normalization factor as

$$\langle\psi|\psi\rangle \simeq \sum_{N_{f\uparrow}N_{f\downarrow}D_{c\uparrow}D_{c\downarrow}} \exp[Lf(n_{f\uparrow}, n_{f\downarrow}, d_{c\uparrow}, d_{c\downarrow})], \tag{17}$$

where $n_{f\sigma} = N_{f\sigma}/L$ and $d_{c\sigma} = D_{c\sigma}/L$. In the summation, the most important terms should satisfy

$$\frac{\partial f(n_{f\uparrow}, n_{f\downarrow}, d_{c\uparrow}, d_{c\downarrow})}{\partial d_{c\sigma}} = 0, \tag{18}$$

and

$$\frac{\partial f(n_{f\uparrow}, n_{f\downarrow}, d_{c\uparrow}, d_{c\downarrow})}{\partial n_{f\sigma}} = 0. \tag{19}$$

From eq. (18), we obtain

$$g^2 = \frac{d_{c\sigma}(1 - n_f - n_{c\sigma} + d_{c\sigma})}{(n_f - d_{c\sigma})(n_{c\sigma} - d_{c\sigma})}, \tag{20}$$

where $n_{c\sigma} = n_{\sigma} - n_{f\sigma}$ with $n_{\sigma} = N_{\sigma}/L$. This is the same form as that in the Hubbard model,²¹⁾ if we regard $n_{c\sigma}$ as n_{σ}^H , n_f as n_{σ}^H , and $d_{c\sigma}$ as d^H , where n_{σ}^H and d^H are the numbers of σ -spin electrons and doubly occupied sites per lattice site, respectively, in the Hubbard model, and $\bar{\sigma}$ denotes the opposite spin of σ . From eq. (19), we obtain

$$e^{\mu(n_{f\sigma})} = \frac{n_f^2(n_{c\sigma} - d_{c\sigma})(1 - n_{c\sigma})(1 - n_f - n_{c\bar{\sigma}} + d_{c\bar{\sigma}})}{(1 - n_{f\sigma})(1 - n_f)n_{c\sigma}(n_f - d_{c\sigma})(n_f - d_{c\bar{\sigma}})}, \tag{21}$$

where μ is the chemical potential for the fictitious system defined as

$$\mu(n_{f\sigma}) = \left. \frac{dF(N)}{dN} \right|_{N=N_{f\sigma}}. \tag{22}$$

In the following, we assume a paramagnetic state, i.e., $n_{f\sigma} = n_f/2$, $n_{c\sigma} = n_c/2 = (n - n_f)/2$, and $d_{c\sigma} = d/2$, and optimize the wave function so that it has the lowest energy. In the following, we regard d as a variational parameter instead of g by using eq. (20). From the definition of the chemical potential in the grand canonical ensemble, the following equation should be satisfied

$$\begin{aligned}
n_f/2 &= \frac{1}{L} \sum_{k < k_F} \frac{1}{1 + e^{-\ln a^2(k) - \mu(n_f/2)}} \\
&= \frac{1}{L} \sum_{k < k_F} \frac{a^2(k)}{q^{-1} + a^2(k)},
\end{aligned} \tag{23}$$

where we have introduced $q = e^{\mu(n_f/2)}$.

If we set $g = 1$, that is, if we ignore the correlation between the conduction and f electrons, we obtain $d = n_c n_f$

and $q^{-1} = (1 - n_f/2)/(1 - n_f)$, which is the renormalization factor given in eq. (1). Our theory is reduced to the previous Gutzwiller method for the PAM by setting $g = 1$. This can also be checked for other quantities, such as renormalization factors, which will be derived in the following.

Next, we evaluate the kinetic energy. The effect of the annihilation operator on the variational wave function is written as

$$\begin{aligned} c_{r'\uparrow}|\psi\rangle &= \sum_{N_{f\uparrow}N_{f\downarrow}} \sum_{\{\mathbf{r}\}|\mathbf{k}^{(f\uparrow)}\rangle} g^D (-1)^{\text{perm}(\{\mathbf{k}^{(f\uparrow)}\})} \\ &\times \prod_{i=1}^{N_{f\uparrow}} a(\mathbf{k}_i^{(f\uparrow)}) \prod_{j=1}^{N_{f\downarrow}} a(\mathbf{k}_j^{(f\downarrow)}) \\ &\times \det^{(r')} [\varphi_{\mathbf{k}^{(e\uparrow)}}(\mathbf{r}^{(e\uparrow)})] \det[\varphi_{\mathbf{k}^{(f\uparrow)}}(\mathbf{r}^{(f\uparrow)})] \\ &\times \det[\varphi_{\mathbf{k}^{(e\downarrow)}}(\mathbf{r}^{(e\downarrow)})] \det[\varphi_{\mathbf{k}^{(f\downarrow)}}(\mathbf{r}^{(f\downarrow)})] \\ &\times |\{\mathbf{r}_1^{(e\uparrow)} \dots \mathbf{r}_{N_{e\uparrow}-1}^{(e\uparrow)}\} \{\mathbf{r}^{(f)}\}|, \end{aligned} \quad (24)$$

where

$$\begin{aligned} &\det^{(r')} [\varphi_{\mathbf{k}^{(e\uparrow)}}(\mathbf{r}^{(e\uparrow)})] \\ &= \begin{vmatrix} \varphi_{\mathbf{k}_1^{(e\uparrow)}}(\mathbf{r}') & \varphi_{\mathbf{k}_1^{(e\uparrow)}}(\mathbf{r}_1^{(e\uparrow)}) \\ \varphi_{\mathbf{k}_2^{(e\uparrow)}}(\mathbf{r}') & \ddots \\ \varphi_{\mathbf{k}_{N_{e\uparrow}}^{(e\uparrow)}}(\mathbf{r}') & \varphi_{\mathbf{k}_{N_{e\uparrow}}^{(e\uparrow)}}(\mathbf{r}_{N_{e\uparrow}-1}^{(e\uparrow)}) \end{vmatrix}. \end{aligned} \quad (25)$$

Thus, we need to introduce another approximation to evaluate the determinant eq. (25). By using eq. (A-10), we obtain, for $\mathbf{r} \neq \mathbf{r}'$,

$$\begin{aligned} \langle \psi | c_{r'\uparrow}^\dagger c_{r'\uparrow} |\psi \rangle &\simeq q_{c\uparrow} \sum_{N_{f\uparrow}N_{f\downarrow}D_{e\uparrow}D_{e\downarrow}} g^{2D} X(N_{f\uparrow}, N_{f\downarrow}) \\ &\times Y(N_f, N_{e\uparrow}, D_{e\uparrow}) Y(N_f, N_{e\downarrow}, D_{e\downarrow}) \\ &\times \sum_{\{\mathbf{k}^{(f\uparrow)}\}} \prod_{i=1}^{N_{f\uparrow}} a^2(\mathbf{k}_i^{(f\uparrow)}) \prod_{j=1}^{N_{f\downarrow}} a^2(\mathbf{k}_j^{(f\downarrow)}) \\ &\times \sum_{l=1}^{N_{e\uparrow}} \varphi_{\mathbf{k}_l^{(e\uparrow)}}^*(\mathbf{r}) \varphi_{\mathbf{k}_l^{(e\uparrow)}}(\mathbf{r}'). \end{aligned} \quad (26)$$

The renormalization factor $q_{c\sigma}$ is given by

$$\begin{aligned} q_c = q_{c\sigma} &= \frac{1}{n_{c\sigma}(1 - n_{c\sigma})} \\ &\times \left[\sqrt{(n_{c\sigma} - d_{c\sigma})(1 - n_f - n_{c\sigma} + d_{c\sigma})} \right. \\ &\left. + \sqrt{d_{c\sigma}(n_f - d_{c\sigma})} \right]^2. \end{aligned} \quad (27)$$

$q_{c\sigma}$ has the same form as the renormalization factor q_σ^H in the Hubbard model²¹⁾ as in the case of the Gutzwiller parameter g . From eq. (26), we can evaluate the momentum distribution function $n_c(\mathbf{k}) = n_{c\uparrow}(\mathbf{k}) = \langle c_{\mathbf{k}\uparrow}^\dagger c_{\mathbf{k}\uparrow} \rangle = \langle \psi | c_{\mathbf{k}\uparrow}^\dagger c_{\mathbf{k}\uparrow} |\psi \rangle / \langle \psi | \psi \rangle$. In this evaluation, we need to calculate $\sum_{\{\mathbf{k}^{(f\uparrow)}\}} \prod_{i=1}^{N_{f\uparrow}} a^2(\mathbf{k}_i^{(f\uparrow)})$ with the restriction $\mathbf{k} \notin \{\mathbf{k}^{(f\uparrow)}\}$. We can accomplish it with the aid of eq. (B-4). The result is

$$n_{c\uparrow}(\mathbf{k}) = \begin{cases} (1 - q_{c\uparrow})n_{c\uparrow} + \Delta n_c(\mathbf{k}) & \text{for } k < k_F \\ (1 - q_{c\uparrow})n_{c\uparrow} & \text{for } k > k_F \end{cases}, \quad (28)$$

where

$$\Delta n_c(\mathbf{k}) = q_c \frac{q^{-1}}{q^{-1} + a^2(\mathbf{k})}. \quad (29)$$

In a similar way, we obtain $n_f(\mathbf{k}) = n_{f\uparrow}(\mathbf{k}) = \langle f_{\mathbf{k}\uparrow}^\dagger f_{\mathbf{k}\uparrow} \rangle$ as

$$n_{f\uparrow}(\mathbf{k}) = \begin{cases} (1 - q_{f\uparrow})n_{f\uparrow} + \Delta n_f(\mathbf{k}) & \text{for } k < k_F \\ (1 - q_{f\uparrow})n_{f\uparrow} & \text{for } k > k_F \end{cases}, \quad (30)$$

where

$$\Delta n_f(\mathbf{k}) = q_f \frac{a^2(\mathbf{k})}{q^{-1} + a^2(\mathbf{k})}. \quad (31)$$

The renormalization factor for an f electron is

$$q_f = q_{f\sigma} = \frac{1 - n_f}{1 - n_{f\sigma}} q_f^{(e\uparrow)} q_f^{(c\downarrow)}, \quad (32)$$

where

$$\begin{aligned} q_f^{(c\sigma)} &= \frac{1}{n_f(1 - n_f)} \\ &\times \left[\sqrt{(n_f - d_{c\sigma})(1 - n_f - n_{c\sigma} + d_{c\sigma})} \right. \\ &\left. + \sqrt{d_{c\sigma}(n_{c\sigma} - d_{c\sigma})} \right]^2. \end{aligned} \quad (33)$$

$q_f^{(c\sigma)}$ has the same form as q_σ^H in the Hubbard model,²¹⁾ if we regard n_f as n_σ^H , $n_{c\sigma}$ as n_σ^H , and $d_{c\sigma}$ as d^H . We can also evaluate the mixing term

$$\langle c_{i\uparrow}^\dagger f_{i\uparrow} \rangle = q_{cf} \frac{1}{L} \sum_{k < k_F} \frac{a(\mathbf{k})}{q^{-1} + a^2(\mathbf{k})}, \quad (34)$$

where the renormalization factor is given by

$$\begin{aligned} q_{cf} = q_{cf\sigma} &= \frac{(n_f - d_{c\sigma})(n_f - d_{c\bar{\sigma}})}{n_f^2(1 - n_{c\sigma})} \\ &\times \left[1 + \sqrt{\frac{d_{c\bar{\sigma}}(n_{c\bar{\sigma}} - d_{c\bar{\sigma}})}{(n_f - d_{c\bar{\sigma}})(1 - n_f - n_{c\bar{\sigma}} + d_{c\bar{\sigma}})}} \right]. \end{aligned} \quad (35)$$

Then, the expectation value of energy $e = \langle H \rangle / L$ per site is given by

$$\begin{aligned} e &= \frac{2}{L} \sum_{k < k_F} \tilde{\epsilon}_k \\ &+ \frac{2}{L} \sum_{k < k_F} \frac{(\epsilon_f - \tilde{\epsilon}_k)a^2(\mathbf{k}) - 2\tilde{V}_1 a(\mathbf{k})}{q^{-1} + a^2(\mathbf{k})} + U_{cf}d, \end{aligned} \quad (36)$$

where $\tilde{\epsilon}_k = q_c \epsilon_k$ and $\tilde{V}_1 = q_{cf} V$. We minimize the expectation value of energy with respect to the variational parameters $a(\mathbf{k})$ and d . From $\partial e / \partial a(\mathbf{k}) = 0$, we obtain

$$a(\mathbf{k}) = \frac{2\tilde{V}_1}{\tilde{\epsilon}_f - \tilde{\epsilon}_k + \sqrt{(\tilde{\epsilon}_f - \tilde{\epsilon}_k)^2 + 4\tilde{V}_2^2}}, \quad (37)$$

where $\tilde{V}_2 = \sqrt{q}\tilde{V}_1$. The renormalized f -level $\tilde{\epsilon}_f$ should satisfy

$$\begin{aligned} \epsilon_f - \tilde{\epsilon}_f = & -2\tilde{V}_2^2 I_2 q \frac{\partial q^{-1}}{\partial n_f} \\ & - (I_1 - I_4 - I_3 \tilde{\epsilon}_f) q_c^{-1} \frac{\partial q_c}{\partial n_f} \\ & + 4\tilde{V}_2^2 I_2 q_{cf}^{-1} \frac{\partial q_{cf}}{\partial n_f}. \end{aligned} \quad (38)$$

The integrals are given by

$$I_1 = \frac{1}{L} \sum_{k < k_F} \tilde{\epsilon}_k, \quad (39)$$

and

$$I_l = \frac{1}{L} \sum_{k < k_F} \frac{(\tilde{\epsilon}_k - \tilde{\epsilon}_f)^{l-2}}{\sqrt{(\tilde{\epsilon}_k - \tilde{\epsilon}_f)^2 + 4\tilde{V}_2^2}}, \quad (40)$$

for $l = 2-4$. From $\partial e / \partial d = 0$, we obtain

$$\begin{aligned} U_{cf} = & -2\tilde{V}_2^2 I_2 q \frac{\partial q^{-1}}{\partial d} \\ & - (I_1 - I_4 - I_3 \tilde{\epsilon}_f) q_c^{-1} \frac{\partial q_c}{\partial d} \\ & + 4\tilde{V}_2^2 I_2 q_{cf}^{-1} \frac{\partial q_{cf}}{\partial d}. \end{aligned} \quad (41)$$

Here, note that while we take $a(\mathbf{k})$ and d as independent variables for $\partial e / \partial a(\mathbf{k}) = 0$ and $\partial e / \partial d = 0$, we take n_f and d as independent variables for the derivatives in eqs. (38) and (41). Equation (23) is rewritten using eqs. (37) and (40) as

$$n_f = \frac{n}{2} + I_3. \quad (42)$$

We solve eqs. (38), (41), and (42), and determine $\tilde{\epsilon}_f$, d , and n_f . By using eqs. (37), (39), and (40), we can rewrite eq. (36) as

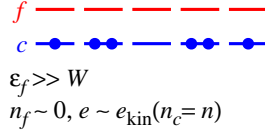
$$e = I_1 + n_f \epsilon_f + \left(\frac{n}{2} - n_f\right) \tilde{\epsilon}_f - I_4 - 4\tilde{V}_2^2 I_2 + U_{cf} d. \quad (43)$$

From the above equations, we find that the band structure of the conduction band is included only through the density of states in the present model, and a physical quantity, such as $n_c(\mathbf{k})$, depends on the momentum \mathbf{k} only through ϵ_k .

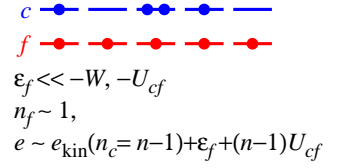
We can evaluate expectation values of physical quantities in the optimized wave function. For example, we obtain the momentum distribution function $n_c(\mathbf{k})$ and $n_f(\mathbf{k})$ using eqs. (28) and (30), respectively. An important quantity is the jump $\Delta n(k_F) = \Delta n_c(k_F) + \Delta n_f(k_F)$ at the Fermi level; its inverse corresponds to the mass enhancement factor. In the following, we call $1/\Delta n(k_F)$ the mass enhancement factor.

In the next section, we show the calculated results for the model with a constant density of states. Before showing them, we discuss three characteristic regimes of the model, schematically presented in Fig. 1, which do not depend on the details of the band structure. First, we consider a case with $\epsilon_f \gg W$ [Fig. 1(a)], where W is a typical energy scale of the conduction band or half of the bandwidth in the next section. In this case, $n_f \simeq 0$ and the energy e per site is almost the same as the kinetic energy $e_{\text{kin}}(n_c)$ per site of the free conduction band with $n_c = n$. Second, we consider a case with $\epsilon_f \ll -W$, $-U_{cf}$ [Fig. 1(b)]. In this case, $n_f \simeq 1$ and $n_c \simeq n - 1$. The energy is

(a) $n_f \simeq 0$ regime



(b) Kondo regime



(c) intermediate-valence regime

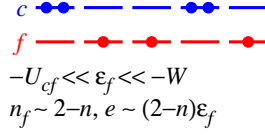


Fig. 1. (Color online) Typical electron configurations in three characteristic regimes: (a) $n_f \simeq 0$ regime, (b) Kondo regime, and (c) intermediate-valence regime. $e_{\text{kin}}(n_c)$ denotes the kinetic energy per site for the free conduction band with n_c .

approximately given by $e \simeq e_{\text{kin}}(n_c = n - 1) + \epsilon_f + (n - 1)U_{cf}$. We call this regime the Kondo regime. For $n_f \rightarrow 1$, we obtain $q \rightarrow 0$, $q_c \rightarrow 1$, $q_f \rightarrow 0$, and $a(k_F)$ diverges as $a(k_F) \sim q^{-1}$. By using them, we find that, for $n_f \rightarrow 1$, $\Delta n_c(k_F) \rightarrow 0$ and $\Delta n_f(k_F) \rightarrow 0$, that is, the mass enhancement factor becomes large. This mass enhancement for $n_f \rightarrow 1$ is consistent with the previous result for the PAM. Third, we consider a case with a moderate ϵ_f and a large U_{cf} , more explicitly, $-U_{cf} \ll \epsilon_f \ll -W$ [Fig. 1(c)]. In this case, f and conduction electrons tend to avoid each other; thus, $n_f + n_c/2 \simeq 1$ and $d \simeq 0$. That is, $n_f \simeq 2 - n$ and $n_c \simeq 2n - 2$. Here, we call this regime the intermediate-valence regime. In this case, both f and conduction electrons are almost localized, and the energy is $e \simeq (2 - n)\epsilon_f$. For $n_f + n_c/2 \rightarrow 1$ and $d \rightarrow 0$, we obtain $q \rightarrow 0$, $q_c \rightarrow 0$, and $q_f \rightarrow 0$. By using them, we can show that the mass enhancement factor becomes large in this intermediate-valence regime. This mass enhancement in the intermediate-valence regime is not realized in the ordinary PAM and is a result of the effect of U_{cf} .

3. Results

Now, we show our calculated results. Here, we consider a simple model for the kinetic energy: the density of states per spin is given by $\rho(\epsilon) = 1/(2W)$ for $-W \leq \epsilon \leq W$; otherwise, $\rho(\epsilon) = 0$.

Figure 2(a) shows n_f as a function of ϵ_f for several U_{cf} values for $V/W = 0.1$ and $n = 1.75$. For a large U_{cf} , we recognize the three regimes mentioned above. A first-order phase transition occurs from the Kondo regime to the intermediate-valence regime or to the $n_f \simeq 0$ regime for $U_{cf}/W > 0.89$. We observe hysteresis by increasing and decreasing ϵ_f across the first-order phase transition point, and here we show the values of the state that has the lower energy. Figure 2(b) shows the number of interacting electron pairs d through U_{cf} per site. For a large U_{cf} , the conduction and f electrons tend to avoid each other and d is suppressed. Figure 2(c) shows the valence susceptibility $\chi_V = -dn_f/d\epsilon_f$ as a function of ϵ_f . The valence susceptibility enhances around the boundaries of three regimes for a large U_{cf} . For $U_{cf} = 0$, such a boundary is not so clear. Figure 2(d) shows the mass enhancement factor $1/\Delta n(k_F)$ as a function of ϵ_f . In addition to the enhancement

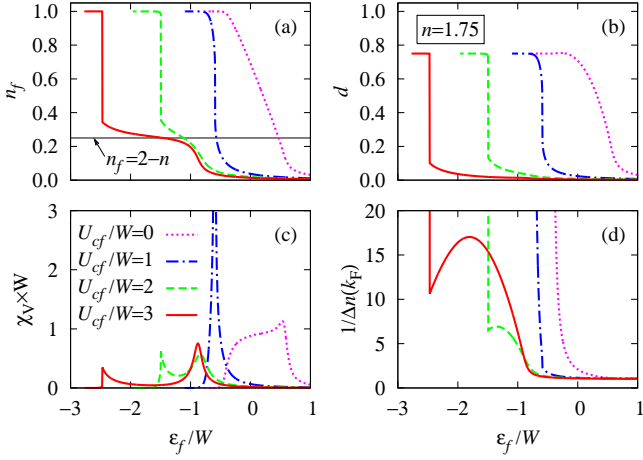


Fig. 2. (Color online) ϵ_f dependences of (a) n_f , (b) d , (c) χ_V , and (d) $1/\Delta n(k_F)$ for $V/W = 0.1$ and $n = 1.75$. $U_{cf}/W = 0$ (dotted lines), 1 (dash-dotted lines), 2 (dashed lines), and 3 (solid lines).

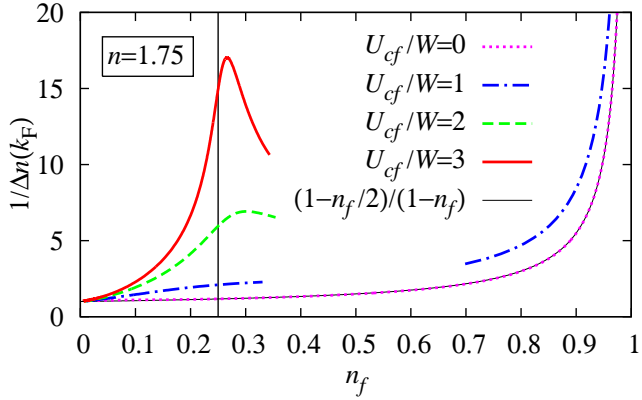


Fig. 3. (Color online) $1/\Delta n(k_F)$ as a function of n_f for $V/W = 0.1$ and $n = 1.75$. $U_{cf}/W = 0$ (dotted lines), 1 (dash-dotted lines), 2 (dashed lines), and 3 (solid lines). The thin line is $(1 - n_f/2)/(1 - n_f)$. The vertical line indicates $n_f = 2 - n$.

for $n_f \rightarrow 1$ as in the ordinary PAM, we find another region, that is, the intermediate-valence regime $n_f \simeq 2 - n$, in which the mass enhancement factor becomes large. This enhancement, in particular, a peak as a function of ϵ_f , is not expected for the PAM without U_{cf} . Our theory may be relevant to the large effective mass in the intermediate-valence compounds α -YbAlB₄ and β -YbAlB₄ and the nonmonotonic variation in the effective mass under pressure in CeCu₂Si₂.

To clearly observe the effect of U_{cf} on the mass enhancement, we show $1/\Delta n(k_F)$ as a function of n_f in Fig. 3. The thin line, which almost overlaps with the $U_{cf} = 0$ data, represents the mass enhancement factor, given by eq. (1), i.e., $(1 - n_f/2)/(1 - n_f)$ obtained for the PAM with $U_{cf} = 0$ and $g = 1$. Note that, in the present theory, $g \neq 1$ even for $U_{cf} = 0$. By increasing U_{cf} , $1/\Delta n(k_F)$ becomes large, particularly in the intermediate-valence regime $n_f \simeq 2 - n$.

In Fig. 4, we show the momentum distribution functions $n_c(\mathbf{k})$ and $n_f(\mathbf{k})$ for $n = 1.75$ and $n_f = 2 - n = 0.25$ for several values of U_{cf} . For $U_{cf} = 0$, the jump at the Fermi energy $\epsilon_{k_F} = (n - 1)W = 0.75W$ is much larger for $n_f(k_F)$ than for $n_c(k_F)$, that is, the quasiparticle weight is mainly composed of the

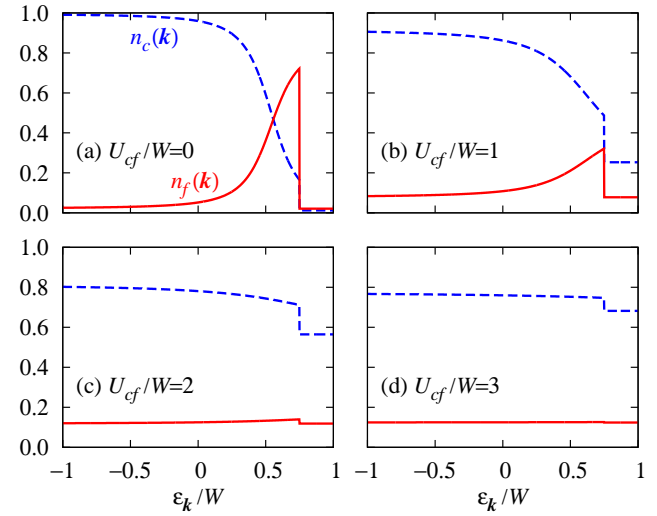


Fig. 4. (Color online) Momentum distribution functions $n_c(\mathbf{k})$ (dashed lines) and $n_f(\mathbf{k})$ (solid lines) as functions of ϵ_k for $V/W = 0.1$, $n = 1.75$, and $n_f = 2 - n = 0.25$. (a) $U_{cf}/W = 0$, (b) $U_{cf}/W = 1$, (c) $U_{cf}/W = 2$, and (d) $U_{cf}/W = 3$.

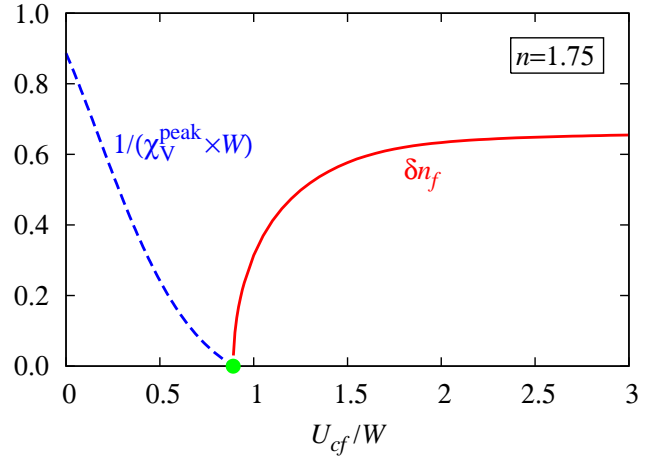


Fig. 5. (Color online) Inverse of peak value χ_V^{peak} (dashed line) of valence susceptibility [see Fig. 2(c)] and jump δn_f (solid line) in n_f [see Fig. 2(a)] at first-order phase transition as functions of U_{cf} for $V/W = 0.1$ and $n = 1.75$. The circle represents the critical point.

f -electron contribution. For a large U_{cf} , the jump becomes small for both $n_f(k_F)$ and $n_c(k_F)$, and the mass enhancement factor becomes large, as shown in Fig. 3.

Figure 5 shows how we determine the critical point of the valence transition. In this figure, we draw the inverse of the peak χ_V^{peak} of the valence susceptibility and the jump δn_f in n_f at the first-order valence transition. Both of them should become zero at the critical point, and indeed, we find that they become zero at the same U_{cf} .

In Fig. 6(a), we show the valence susceptibility χ_V as a function of ϵ_f and U_{cf} for $n = 1.75$. In this figure, we also draw the first-order valence transition line and its critical point. The crossover lines, represented by the dotted lines, are determined by comparing the energies of the three extreme states: $n_f = 0$, $n_f = 1$, and $n_f + n_c/2 = 1$ with $d = 0$. The

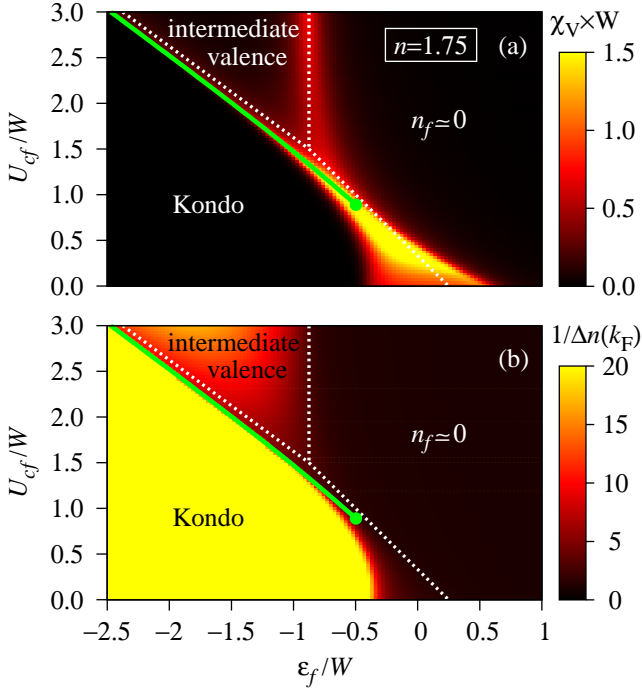


Fig. 6. (Color online) (a) χ_V and (b) $1/\Delta n(k_F)$ as functions of ϵ_f and U_{cf} for $n = 1.75$ with $V/W = 0.1$. The solid lines represent the first-order valence transition line. The solid circles denote the critical point of the valence transition. The dotted lines indicate crossover lines determined by comparing the energies of the three extreme states (see text).

crossover lines are given by

$$\epsilon_f = -(n-1)U_{cf} + e_{\text{kin}}(n_c = n) - e_{\text{kin}}(n_c = n-1), \quad (44)$$

between the Kondo and $n_f \approx 0$ regimes, by

$$\epsilon_f = \frac{e_{\text{kin}}(n_c = n)}{2-n}, \quad (45)$$

between the intermediate-valence and $n_f \approx 0$ regimes, and by

$$\epsilon_f = -U_{cf} - \frac{e_{\text{kin}}(n_c = n-1)}{n-1}, \quad (46)$$

between the Kondo and intermediate-valence regimes. The crossover line between the intermediate-valence and $n_f \approx 0$ regimes does not depend on U_{cf} . The other crossover lines are straight lines with finite slopes. Between the Kondo and $n_f \approx 0$ regimes, the slope is $-1/(n-1)$ and does not depend on the band structure. Between the Kondo and intermediate-valence regimes, the slope is -1 independent of both the band structure and filling n .⁷⁾ The region where χ_V becomes large is captured well by the crossover lines obtained by such a simple consideration. The first-order valence transition occurs only from the Kondo to intermediate-valence or to $n_f \approx 0$ regimes within the U_{cf} range presented here. Note that the valence transition can occur also between the intermediate-valence regime and the $n_f \approx 0$ regime for a smaller n .²⁰⁾ Figure 6(b) shows the mass enhancement factor $1/\Delta n(k_F)$ as a function of ϵ_f and U_{cf} . A large mass enhancement occurs in the intermediate-valence regime in addition to the Kondo regime. Here, note that the large mass enhancement occurs in the middle of the intermediate-valence regime. Thus, this enhancement is not due to valence fluctuations. In CeCu_2Si_2 ,

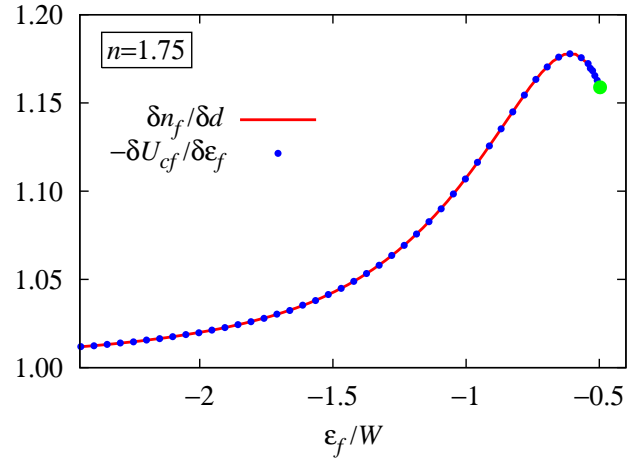


Fig. 7. (Color online) Ratio $\delta n_f/\delta d$ (solid line) of jumps [see Figs. 2(a) and 2(b)] at the first-order phase transition and slope $-\delta U_{cf}/\delta \epsilon_f$ (small circles) of first-order phase transition line (see Fig. 6) for $V/W = 0.1$ and $n = 1.75$. The large circle indicates the critical point.

the effective mass has a peak before the superconducting transition temperature becomes maximum under pressure, and which is consistent with our theory provided that the pairing interaction of superconductivity is mediated by the valence fluctuations. The situation will also be similar for CeCu_2Ge_2 if we can subtract the contributions of magnetic fluctuations.

Finally, to verify the consistency of the present theory, we check the Clausius-Clapeyron relation for the first-order valence transition.^{7,22)} This relation is given by

$$\frac{\delta n_f}{\delta d} = -\frac{\delta U_{cf}}{\delta \epsilon_f}, \quad (47)$$

where δd denotes the jump in d at the valence transition, and $\delta U_{cf}/\delta \epsilon_f$ is the slope of the valence transition line. In Fig. 7, we show the values of the quantities on the left and right sides of eq. (47). We can clearly see that the Clausius-Clapeyron relation holds in the present theory. Note that the Clausius-Clapeyron relation also holds for the crossover lines mentioned above. For example, $n_f \approx 1$ and $d \approx n-1$ for the Kondo regime and $n_f \approx 0$ and $d \approx 0$ for the $n_f \approx 0$ regime, and then, between these two regimes, $\delta n_f/\delta d \approx 1/(n-1)$. It is the slope $-\delta U_{cf}/\delta \epsilon_f$ for that crossover line given by eq. (44).

4. Summary and Discussion

We have studied the extended periodic Anderson model with U_{cf} by Gutzwiller approximation. We have found that the three regimes, that is, the Kondo, intermediate-valence, and $n_f \approx 0$ regimes, are clearly defined for a large U_{cf} . Then, we have found that, in the intermediate-valence regime, the effective mass is enhanced substantially. According to the present theory, the large mass enhancement in the intermediate-valence regime indicates a large U_{cf} . Thus, our theory provides helpful information for searching a superconductor with valence-fluctuation-mediated pairing.

In this study, we have not considered the possible instability toward a spin-density-wave state and a charge-density-wave state. Such a state would be realized in a portion of the parameter space, particularly, in a lattice without geometric frustration.^{8,19)} The extension of the present theory to such

states is a future problem. In the present theory for a uniform state, the effect of a lattice structure is included only through the density of states of the conduction band. Thus, our results may change little for a frustrated lattice with a similar density of states even if we consider the possibility of the density-wave states.

In our theory, we expand both the conduction- and f -electron states in the basis states in real space; thus, it will be possible to include the onsite correlation between conduction electrons and other short-range correlations. These extensions are future problems.

Acknowledgment

This work is supported by a Grant-in-Aid for Young Scientists (B) from the Japan Society for the Promotion of Science.

Appendix A: Approximation for Determinants

In this appendix, we introduce approximations for determinants to evaluate expectation values in the variational wave function. Although most of them have been derived in ref. 10, we repeat them for the readers' convenience.

We consider the state

$$|\mathbf{k}_1 \cdots \mathbf{k}_N\rangle = c_{\mathbf{k}_1}^\dagger \cdots c_{\mathbf{k}_N}^\dagger |0\rangle, \quad (\text{A-1})$$

where $c_{\mathbf{k}_i}^\dagger$ denotes the creation operator of a spinless fermion with the momentum \mathbf{k}_i . From eq. (8), we obtain

$$\begin{aligned} & \langle \mathbf{k}'_1 \cdots \mathbf{k}'_N | \mathbf{k}_1 \cdots \mathbf{k}_N \rangle \\ &= \sum_{\{\mathbf{r}\}} \det[\varphi_{\mathbf{k}'_i}^*(\mathbf{r})] \det[\varphi_{\mathbf{k}_i}(\mathbf{r})] \\ &= \delta_{\mathbf{k}'_1 \mathbf{k}_1} \cdots \delta_{\mathbf{k}'_N \mathbf{k}_N}. \end{aligned} \quad (\text{A-2})$$

Then, we approximate each product of determinants by the average, that is,

$$|\det[\varphi_{\mathbf{k}}(\mathbf{r})]|^2 \simeq \frac{1}{LC_N}, \quad (\text{A-3})$$

and

$$\det[\varphi_{\mathbf{k}'}^*(\mathbf{r})] \det[\varphi_{\mathbf{k}}(\mathbf{r})] \simeq 0, \quad (\text{A-4})$$

for $\{\mathbf{k}\} \neq \{\mathbf{k}'\}$.

For the kinetic energy, we need to evaluate another type of determinant. We consider

$$\begin{aligned} c_{\mathbf{r}'} |\mathbf{k}_1 \cdots \mathbf{k}_N\rangle &= \sum_{\{\mathbf{r}\}} \det[\varphi_{\mathbf{k}}(\mathbf{r})] c_{\mathbf{r}'} |\mathbf{r}_1 \cdots \mathbf{r}_N\rangle \\ &= \sum_{\{\mathbf{r}\} \neq \mathbf{r}'} \det^{(\mathbf{r}')}[\varphi_{\mathbf{k}}(\mathbf{r})] |\mathbf{r}_1 \cdots \mathbf{r}_{N-1}\rangle, \end{aligned} \quad (\text{A-5})$$

where

$$\det^{(\mathbf{r}')}[\varphi_{\mathbf{k}}(\mathbf{r})] = \begin{vmatrix} \varphi_{\mathbf{k}_1}(\mathbf{r}') & \varphi_{\mathbf{k}_1}(\mathbf{r}_1) & & \\ \varphi_{\mathbf{k}_2}(\mathbf{r}') & & \ddots & \\ & & & \varphi_{\mathbf{k}_N}(\mathbf{r}_{N-1}) \end{vmatrix}. \quad (\text{A-6})$$

Then, for $\mathbf{r}' \neq \mathbf{r}''$,

$$\begin{aligned} & \langle \mathbf{k}_1 \cdots \mathbf{k}_N | c_{\mathbf{r}'}^\dagger c_{\mathbf{r}''} | \mathbf{k}_1 \cdots \mathbf{k}_N \rangle \\ &= \sum_{\{\mathbf{r}\} \neq \mathbf{r}', \mathbf{r}''} \det^{(\mathbf{r}')}[\varphi_{\mathbf{k}}^*(\mathbf{r})] \det^{(\mathbf{r}'')}[\varphi_{\mathbf{k}}(\mathbf{r})]. \end{aligned} \quad (\text{A-7})$$

On the other hand, by using the expansion

$$c_{\mathbf{r}'} = \sum_{\mathbf{k}'} \varphi_{\mathbf{k}'}(\mathbf{r}') c_{\mathbf{k}'}, \quad (\text{A-8})$$

we obtain

$$\begin{aligned} & \langle \mathbf{k}_1 \cdots \mathbf{k}_N | c_{\mathbf{r}'}^\dagger c_{\mathbf{r}''} | \mathbf{k}_1 \cdots \mathbf{k}_N \rangle \\ &= \sum_{\mathbf{k}'} \varphi_{\mathbf{k}'}^*(\mathbf{r}') \varphi_{\mathbf{k}'}(\mathbf{r}'') \langle \mathbf{k}_1 \cdots \mathbf{k}_N | c_{\mathbf{k}'}^\dagger c_{\mathbf{k}'} | \mathbf{k}_1 \cdots \mathbf{k}_N \rangle \\ &= \sum_{i=1}^N \varphi_{\mathbf{k}_i}^*(\mathbf{r}') \varphi_{\mathbf{k}_i}(\mathbf{r}''). \end{aligned} \quad (\text{A-9})$$

Then, we approximate the products of determinants in eq. (A-7) by their average:

$$\begin{aligned} & \det^{(\mathbf{r}')}[\varphi_{\mathbf{k}}^*(\mathbf{r})] \det^{(\mathbf{r}'')}[\varphi_{\mathbf{k}}(\mathbf{r})] \\ & \simeq \frac{1}{L-2C_{N-1}} \sum_{i=1}^N \varphi_{\mathbf{k}_i}^*(\mathbf{r}') \varphi_{\mathbf{k}_i}(\mathbf{r}''). \end{aligned} \quad (\text{A-10})$$

Appendix B: Evaluation of $\sum \prod a^2(\mathbf{k})$ with Restriction

In the canonical ensemble for an N free-electron system with dispersion $\varepsilon_{\mathbf{k}}$ at temperature $1/\beta$, the hole distribution function is given by

$$\langle c_{\mathbf{k}} c_{\mathbf{k}}^\dagger \rangle = \sum_{\{\mathbf{k}'\} \neq \mathbf{k}} e^{-\beta \sum_{i=1}^N \varepsilon_{\mathbf{k}'_i}} / Z(N), \quad (\text{B-1})$$

where $Z(N)$ is the partition function. It should be equivalent to that in the grand canonical ensemble,

$$\frac{e^{\beta(\varepsilon_{\mathbf{k}} - \mu)}}{1 + e^{\beta(\varepsilon_{\mathbf{k}} - \mu)}}, \quad (\text{B-2})$$

where μ is the chemical potential, and thus,

$$\sum_{\{\mathbf{k}'\} \neq \mathbf{k}} e^{-\beta \sum_{i=1}^N \varepsilon_{\mathbf{k}'_i}} = \frac{e^{-\beta \mu}}{e^{-\beta \mu} + e^{-\beta \varepsilon_{\mathbf{k}}}} Z(N). \quad (\text{B-3})$$

By putting $\varepsilon_{\mathbf{k}} = -\ln a^2(\mathbf{k})$, $\beta = 1$, and $e^\mu = q$, we obtain

$$\sum_{\{\mathbf{k}'\} \neq \mathbf{k}} \prod_{i=1}^N a^2(\mathbf{k}'_i) = \frac{q^{-1}}{q^{-1} + a^2(\mathbf{k})} Z(N). \quad (\text{B-4})$$

-
- 1) F. Steglich, J. Aarts, C. D. Bredl, W. Lieke, D. Meschede, W. Franz, and H. Schäfer: Phys. Rev. Lett. **43** (1979) 1892.
 - 2) B. Bellarbi, A. Benoit, D. Jaccard, J. M. Mignot, and H. F. Braun: Phys. Rev. B **30** (1984) 1182.
 - 3) E. Vargoz and D. Jaccard: J. Magn. Magn. Mater. **177–181** (1998) 294.
 - 4) H. Q. Yuan, F. M. Grosche, M. Deppe, C. Geibel, G. Sparn, and F. Steglich: Science **302** (2003) 2104.
 - 5) K. Miyake, O. Narikiyo, and Y. Onishi: Physica B **259–261** (1999) 676.
 - 6) Y. Onishi and K. Miyake: J. Phys. Soc. Jpn. **69** (2000) 3955.
 - 7) S. Watanabe, M. Imada, and K. Miyake: J. Phys. Soc. Jpn. **75** (2006) 043710.
 - 8) T. Sugibayashi, Y. Saiga, and D. S. Hirashima: J. Phys. Soc. Jpn. **77** (2008) 024716.
 - 9) T. M. Rice and K. Ueda: Phys. Rev. B **34** (1986) 6420.
 - 10) P. Fazekas and B. H. Brandow: Phys. Scr. **36** (1987) 809.
 - 11) D. Jaccard, H. Wilhelm, K. Alami-Yadri, and E. Vargoz: Physica B **259–261** (1999) 1.
 - 12) A. T. Holmes, D. Jaccard, and K. Miyake: Phys. Rev. B **69** (2004) 024508.
 - 13) J.-P. Rueff, S. Raymond, M. Taguchi, M. Sikora, J.-P. Itié, F. Baudalet,

- D. Braithwaite, G. Knebel, and D. Jaccard: Phys. Rev. Lett. **106** (2011) 186405.
- 14) R. T. Macaluso, S. Nakatsuji, K. Kuga, E. L. Thomas, Y. Machida, Y. Maeno, Z. Fisk, and J. Y. Chan: Chem. Mater. **19** (2007) 1918.
- 15) M. Okawa, M. Matsunami, K. Ishizaka, R. Eguchi, M. Taguchi, A. Chainani, Y. Takata, M. Yabashi, K. Tamasaku, Y. Nishino, T. Ishikawa, K. Kuga, N. Horie, S. Nakatsuji, and S. Shin: Phys. Rev. Lett. **104** (2010) 247201.
- 16) C. E. T. Gonçalves da Silva and L. M. Falicov: Solid State Commun. **17** (1975) 1521 .
- 17) Y. Onishi and K. Miyake: Physica B **281–282** (2000) 191.
- 18) Y. Saiga, T. Sugibayashi, and D. S. Hirashima: J. Phys. Soc. Jpn. **77** (2008) 114710.
- 19) T. Yoshida, T. Ohashi, and N. Kawakami: J. Phys. Soc. Jpn. **80** (2011) 064710.
- 20) K. Kubo: J. Phys. Soc. Jpn. **80** (2011) 063706.
- 21) M. C. Gutzwiller: Phys. Rev. **137** (1965) A1726.
- 22) S. Watanabe and M. Imada: J. Phys. Soc. Jpn. **73** (2004) 3341.